The pore radius distribution in paper. Part I: The effect of formation and grammage

C.T.J. Dodson* A.G. Handley† Y. Oba‡ W.W. Sampson§

June 10, 2002

Abstract

The pore radius distribution in paper is known to be influenced by changes in the mean grammage and formation. Experimental data are presented that confirm the established result that the standard deviation of pore radii is proportional to the mean. The data show also that this proportionality is the same for changes in grammage and formation and that, contrary to results reported in the literature, the coefficient of variation of pore radii is approximately constant. This property of the pore radius distribution confirms that the gamma distribution is appropriate for its characterisation. We find that the mean pore radius increases with worsening formation but the effect is weak compared to that of changing grammage. Of the formation indices examined, the mean pore radius is most strongly correlated to a weighted index of floc grammage.

Introduction

The pore radius distribution in paper was shown by Corte and Lloyd [1] to be approximately lognormal in shape and to be sensitive to changes in formation. They found the standard deviation of pore radius to be proportional to its mean with higher values being associated with poor formation. The experimental technique used by Corte and Lloyd and the theoretical background was described earlier by Corte [2]. The influence of sheet grammage on the pore radius distribution, measured using Corte's method, was studied by Bliesner [3] for pads of grammage between 50 $g\,m^{-2}$ and 150 $g\,m^{-2}$. Again, the standard deviation of pore radius was found to be proportional to the mean and values decreased with increasing grammage.

Expressions for the pore radius distribution in random fibre networks were derived by Corte and Lloyd [1]. As the mean number of sides per polygon in a random network of lines is four and the distances between crossings are distributed according to the exponential distribution [4], Corte and Lloyd derived the probability density function for rectangular pore areas and hence that for the radii of circles having the same area. Their derivation showed, in agreement with experimental observation, the pore radius distribution to be lognormal in shape and the standard deviation of pore radii to be proportional to the mean.

Dodson and Sampson [5] observed however that such good agreement between theory and experiment is somewhat surprising as, by changing the formation of the sheets they studied, Corte and Lloyd had ensured that their structures were non-random. They rederived the theory of

*Department of Mathematics, UMIST, PO Box 88, Manchester, M60 1QD, UK. *dodson@umist.ac.uk*

†Department of Paper Science, UMIST, PO Box 88, Manchester, M60 1QD, UK. *a.g.handley@umist.ac.uk*

‡Oji Paper Company Ltd., 1-10-6 Shinonome, Koto, Tokyo, 135-8558, Japan. *yasuhiro-oba@ojipaper.co.jp*

§Corresponding Author. Department of Paper Science, UMIST, PO Box 88, Manchester, M60 1QD, UK. *w.sampson@umist.ac.uk*

Corte and Lloyd by representing the distances between crossings in a fibre network by the gamma distribution which has probability density,

$$f(x) = \frac{b^k}{\Gamma(k)} x^{k-1} e^{-b\ x} \quad , \tag{1}$$

with mean, $\bar{x} = k/b$ and variance, $\sigma^2(x) = k/b^2$. On this basis, Dodson and Sampson give the probability density function for pore radii, r as,

$$g(r) = \frac{4\, b^{2\,k}\, \pi^k\, r^{2\,k-1}\, K_0(z)}{\Gamma(k)^2)} \tag{2}$$

where $z = 2\, b\, r\, \sqrt{\pi}$ and $K_0(z)$ is the zeroth order modified Bessel function of the second kind. The mean and variance of pore radii are given by,

$$\bar{r} \quad = \quad \frac{\Gamma(k+\frac{1}{2})^2}{b\,\sqrt{\pi}\,\Gamma(k)^2} \tag{3}$$

$$\sigma^2(r) \quad = \quad \bar{r}^2 \left(\frac{k^2\,\Gamma(k)^4}{\Gamma(k+\frac{1}{2})^4} - 1 \right). \tag{4}$$

Thus, the mean and variance of pore radii, are characterised by the two parameters of the gamma distribution; we note also that the probability density of pore radii given by Equation (2) is itself closely approximated by a gamma distribution and that, in comparison with the distributions of Corte and Lloyd [1] and those of Bliesner [3], the pore radius distribution exhibited similar shape and skewness to a lognormal distribution with the same mean and variance. Since the exponential distribution is a special case of the gamma distribution when $k = 1$, the pore radius theory of Dodson and Sampson includes the random case of Corte and Lloyd as a special case. We note that the probability density function given by Equation (2) is itself closely approximated by a gamma distribution with $k \mapsto \frac{1}{2}\left((16k^2+1)^{\frac{1}{2}} - 1\right)$ and $b \mapsto 2\,b\,\sqrt{\pi}$.

The appropriateness of the gamma distribution to characterise pore radii in non-random fibre networks is reinforced by the recent work of Castro and Ostoja-Starzewski [6] who found that area frequency of the radii of inscribed circles touching three sides of a polygon in a random network have a gamma distribution. Also, the number frequency of inscribed circle radii in a random fibre network was shown by Miles [4] to have an exponential distribution. Also, Johnston [7, 8] has shown that pore radius distribution in granular packings is often well described y the gamma distribution.

The results of Corte and Lloyd [1] and those of Bliesner [3] show that changes in formation and grammage each alter the distribution of pore radii such that the standard deviation is proportional to the mean. Here, we present an experimental investigation designed to determine how these proportionalities depend upon each variable. Also, Corte and Lloyd performed only a qualitative assessment of formation; here, several formation statistics have been determined and relationships are investigated between these and the descriptors of the pore radius distribution.

Experimental

Handsheets were formed in a British Standard Sheet Former from a TMP, a Chemical Softwood pulp and a 50:50 blend of the two fibres. Fibre length and coarseness were measured for each pulp using a Kajaani FS-200 fibre length analyser, fibre width was measured using a light microscope with a calibrated graticule. Fibre data are summarised in Table 1.

	Measured			Calculated	
	Mean width, $\bar{\omega}$	Mean Length, λ	Coarseness, δ	Grammage, β_f	Mass, m_f
	μm	mm	$g\,m^{-1} \times 10^4$	$g\,m^{-2}$	μg
TMP	36.5	1.98	2.22	6.08	0.440
Chem.	38.7	2.41	1.16	3.00	0.280
Blend	37.8	2.29	1.69	4.47	0.387

Table 1: Properties of fibres used to prepare sheets

Variable	Conditions	Number
Furnish	TMP Chem. S/W. Blend	3
Consistency (%)	0.071 0.085	2
Settling time (s)	10 30 60 120	4
Grammage ($g\,m^{-2}$)	20 40 60	3
Total Conditions		72

Table 2: Sheet forming conditions.

Standard handsheets were formed from each furnish. Flocculated sheets were formed for each furnish by increasing the time between stirring and forming and by increasing the consistency in the forming chamber to five times the standard. In all, 72 sets of handsheets were formed; conditions are summarised in Table 2. The samples formed at nominal grammages of 40 $g\,m^{-2}$ and 60 $g\,m^{-2}$ are those used in a recently reported study of thickness, mass and density distribution [9].

The pore radius distribution was measured using a capillary flow porometer, model CFP1500 AEX manufactured by PMI Inc. The instrument automates the saturated head gas drive technique described by Corte [2] and conforms to ASTM standards [10]. The instrument is provided with proprietary software giving, for example, flow weighted mean pore radius and filtration characteristics. Of interest in this study is the number frequency pore radius distribution; accordingly we have used the instrument to record the flow rate of dry air at a given pressure and have applied the equations of Corte [2] to determine this property of the sheets. The saturating fluid used was a silicon oil of surface tension 20.6 $mN\,m^{-1}$. For each condition, the pore radius distribution was determined from the average pressure-flow response of three samples; a circular area of diameter 12 mm was used for each repeat.

Formation was measured using β-radiography and image analysis following the technique described by Sampson [11].

Results and discussion

Examples of pore size distributions are shown in Figure 1 for 60 $g\,m^{-2}$ sheets with good and poor formation formed from the chemical softwood pulp. The graphs show also the quality of fit given by a gamma distribution with the same mean and variance as the data. The quality of the fits are

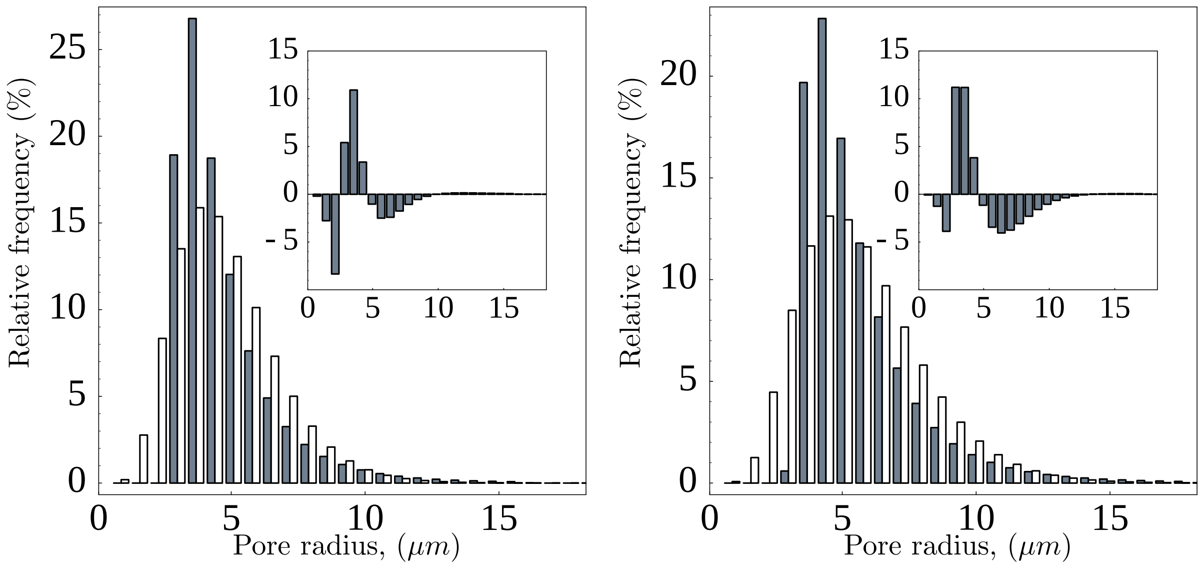

Figure 1: Example frequency distributions of pore radii (grey bars) with comparison with best fit to gamma distributions (white bars). Data shown for 60 $g\,m^{-2}$ sheets formed from chemical softwood fibres. Left: Standard handsheets ($\bar{r} = 4.2$ μm, $CV(r) = 45.3$ %); Right: 60 s settling time before drainage and high initial suspension consistency ($\bar{r} = 5.1$ μm, $CV(r) = 44.9$ %). Inset figures show the difference between real and fitted data.

good and these are typical of our data.

The standard deviation of pore radii, $\sigma(r)$ is plotted against the mean pore radius, $\bar{r}$ in Figure 2. For clarity the data in the bottom left and top right has been plotted on expanded scales; in these plots the solid lines represent a linear regression on the data in the plot, and the broken lines represent a linear regression on the full data set. Full regression data is given in Table 3. In agreement with the observations of Bliesner [3] for changes in grammage, and those of Corte and Lloyd for [1] for changes in formation, the data show a clear proportionality between the standard deviation of pore radius and the mean and the mean pore radius decreases with increasing grammage. Importantly however, the data shows that changes in grammage and formation cause the mean and standard deviation of pore radius to move along the *same* line; also, for our fibres of similar width, but with different mean lengths and coarsenesses, the proportionality is rather insensitive to fibre type.

Inspection of the data plotted on the expanded scales shows that at a nominal grammage of 20 $g\,m^{-2}$, the largest mean pore radii are found in the sheets formed from the TMP. Sheets formed from the Chemical and blended furnishes have smaller mean pore radii and the correlation between the standard deviation and mean is weak; nevertheless, the data for these sheets form a tight cluster about the regression line. There is some overlap in the observed ranges of the mean and hence standard deviation of pore radii for the samples formed at nominal grammages of 40 and 60 $g\,m^{-2}$ though the samples formed at a nominal grammage of 20 $g\,m^{-2}$ form a separate group. This is likely to be due to the large number of pinholes or 'through-pores' at the lowest grammage.

For a random sheet, we can calculate the occurrence of pinholes as the fraction of the sheet where the fibre coverage is zero; this is given by the Poisson distribution as,

$$P(0) = e^{-\frac{\bar{\beta}}{\beta_f}} \quad , \tag{5}$$

where $\bar{\beta}$ is the mean sheet grammage ($g\,m^{-2}$) and β_f is the mean fibre grammage ($g\,m^{-2}$) as given in Table 1. At a nominal sheet grammage of 20 $g\,m^{-2}$ this corresponds to a probability of 3.7 % for the TMP, 1.1 % for the blend and 0.1 % for the chemical pulp. At 40 $g\,m^{-2}$, these probabilities reduce to 0.1 % for the TMP and are negligible for the blend and the chemical pulp.

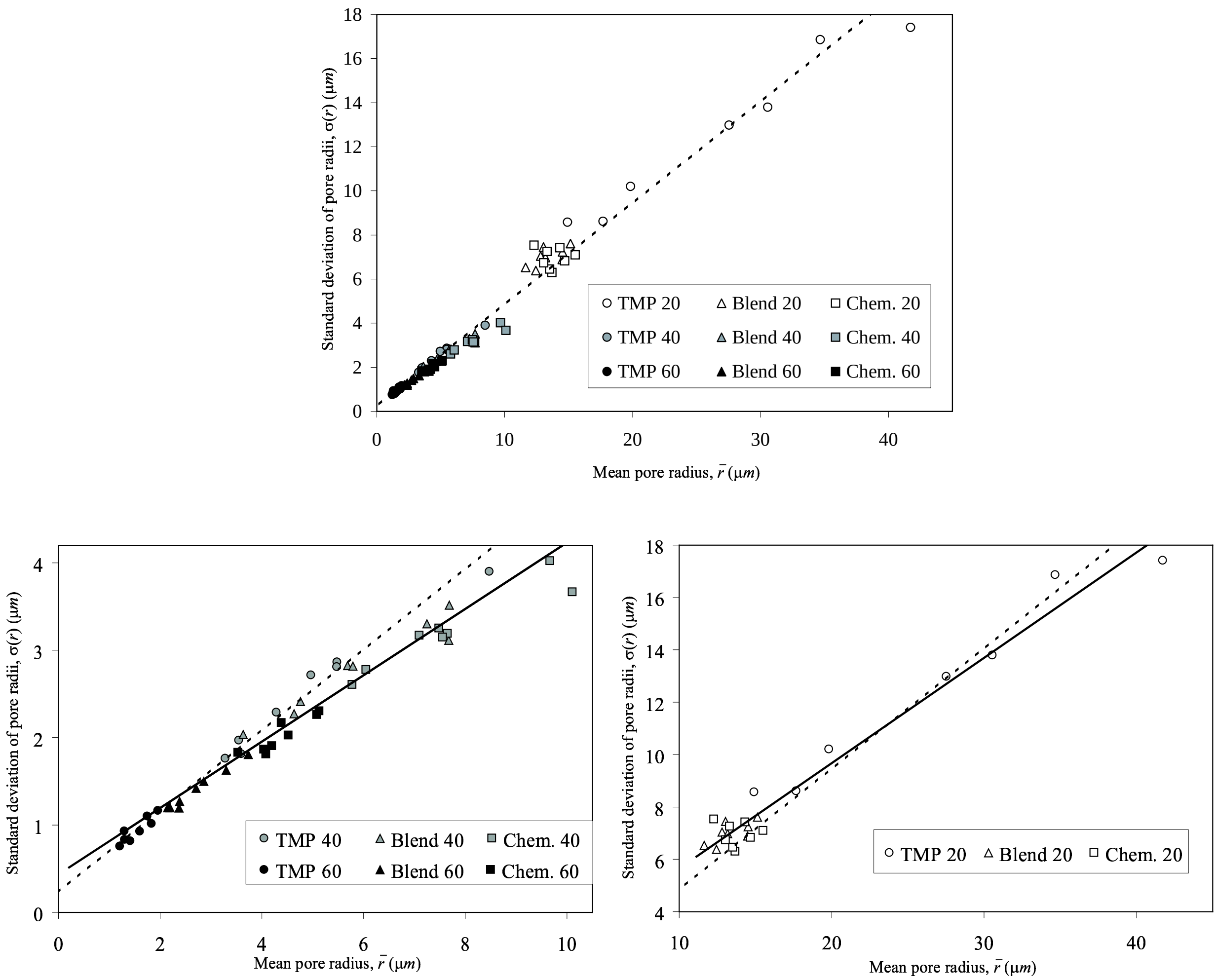

Figure 2: Standard deviation of pore radius plotted against mean pore radius. Top: full grammage range; bottom left: nominal grammage 40 and 60 $g\,m^{-2}$; bottom right: nominal grammage 20 $g\,m^{-2}$. Legends give furnish and nominal mean grammage; broken lines represent linear regression on full data set; solid lines represent linear regression on data in plot.

		Gradient	Intercept	r^2	n
		–	μm	–	
TMP	20 $g\,m^{-2}$	0.369	2.781	0.964	7
	40 $g\,m^{-2}$	0.418	0.471	0.975	8
	60 $g\,m^{-2}$	0.464	0.226	0.817	8
Blend	20 $g\,m^{-2}$	0.245	3.723	0.481	8
	40 $g\,m^{-2}$	0.328	0.852	0.938	8
	60 $g\,m^{-2}$	0.404	0.307	0.980	8
Chem.	20 $g\,m^{-2}$	-0.039	7.485	0.008	8
	40 $g\,m^{-2}$	0.279	1.087	0.900	8
	60 $g\,m^{-2}$	0.336	0.553	0.822	8
All grammages	TMP	0.446	0.407	0.989	23
	Blend	0.519	0.073	0.981	24
	Chem.	0.511	-0.340	0.942	24
All furnishes	20 $g\,m^{-2}$	0.402	1.627	0.966	23
	40 $g\,m^{-2}$	0.312	0.923	0.922	24
	60 $g\,m^{-2}$	0.381	0.358	0.983	24
Overall		0.462	0.233	0.978	71

Table 3: Regression of $\sigma(r)$ on $\bar{r}$.

For flocculated sheets we expect there to be a greater likelihood of pinholes; however, the figures for random networks provide a basis for comparison and are consistent with the data obtained at low grammages.

For the sheets formed with a nominal grammage of 60 $g\,m^{-2}$, the smallest mean pore radii are observed in the sheets formed from the TMP, the largest with the chemical softwood and the values for the blended furnish fall inbetween. At 40 $g\,m^{-2}$ there is no clear boundary between the type of furnish and the range of mean pore radii observed.

Coefficient of variation

The data in Figure 2 show that the relationship between mean pore radius and the standard deviation of pore radii is linear for changes in grammage and formation and that the intercept is close to zero. Since the coefficient of variation of pore radii is given by the standard deviation divided by the mean, it follows that if the intercept is precisely zero then the coefficient of variation of pore radii is constant. In fact, since pore radii are real and positive then, as the mean pore radius tends to zero, so must the standard deviation of pore radii. We expect therefore that for the data presented here the coefficient of variation of pore radii will be approximately constant; for more detailed discussion of this and its relevance to gamma and lognormally distributed variables see [12].

The coefficient of variation of pore radii, $CV(r)$ is plotted against the mean pore radius in Figure 3; the broken lines represent log-linear regressions on the data for 40 $g\,m^{-2}$, 60 $g\,m^{-2}$ and the two groups of data at 20 $g\,m^{-2}$. The broken horizontal line represents the mean coefficient of variation of pore radii observed across all data sets. Although the data show the coefficient of variation of pore radii to decrease with increasing mean pore radii at a given mean grammage, each fibre *type* within these groups exhibits a very narrow range of coefficients of variation of pore radii. The strongest trend in Figure 3 is observed for the TMP fibres at a mean grammage of 20 $g\,m^{-2}$ where there is a very broad range of mean pore radii and this is likely to be attributable to the occurrence of pinholes as discussed previously.

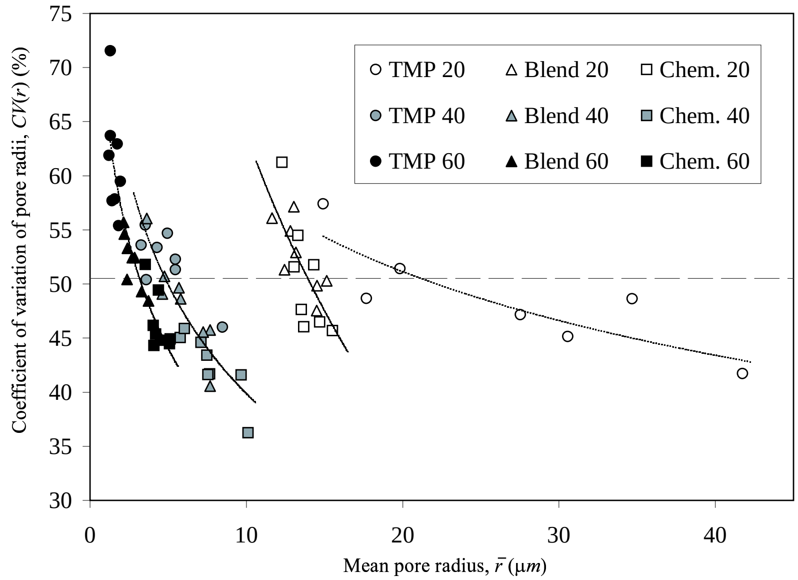

Figure 3: Coefficient of variation of pore radii plotted against mean pore radius. At a given grammage, an increase in mean pore radius is associated with a decrease in the coefficient of variation of pore radii.

The decrease in coefficient of variation of pore radii with increasing mean pore radius shown in Figure 3 arises from the small positive intercept of the regressions given in Table 3. As discussed above, the relationship between standard deviation of pore radii and the mean pore radius must pass through the origin. As such we would expect the standard deviation of pore radii for samples with smaller mean than those analysed here to be less than that predicted by the regressions given in Table 3. Assuming the relationship between the standard deviation of pore radii and the mean pore radius to be monotonic and to exhibit no inflexion, this permits two possibilities for the behaviour at small mean pore radii. Firstly, the standard deviation of pore radii may increase with increasing mean pore radius but with a decreasing gradient until this becomes approximately constant and equal to that given by the regression equations. Alternatively, there may be a small and systematic underestimate in the data such that the observed gradients are correct and the relationship passes through the origin. Identification of the precise behaviour of the relationship in this region requires further experimentation. However, for the range of pore sizes observed here, linear fits to the data are good and it is reasonable to expect this to persist at smaller pore radii. Note also that the theory associated with with the measurement technique assumes pores to be cylindrical and this may cause an underestimate of pore radius. The data of Corte and Lloyd [1] and Bliesner [3] exhibit a negative intercept and this is consistent with an overestimate of pore radii. The fact that our data yields an intercept closer to the origin is likely to be due to the greater experimental control and automation available through advances in technology.

We state therefore that the relationship between the standard deviation of pore radii and the mean pore radius is linear and passes close to the origin for changes in mean sheet grammage and formation. A consequence of the small positive intercept observed is that the coefficient of variation of pore radii decreases with increasing mean pore radius. For sheets formed at a given grammage from a given pulp type, this decrease is weak and, to a first approximation the coefficient of variation of pore radii may be considered constant. This result is in direct contrast to the findings of Corte and Lloyd [1] and Bliesner [3].

It has been recently shown also that if the coefficient of variation of random variables is independent of their mean then the variables have a gamma distribution [13]. Our data therefore confirm the suitability of the gamma distribution to characterise the pore size distribution in paper and therefore reinforce the assumptions made in the model of Dodson and Sampson [5].

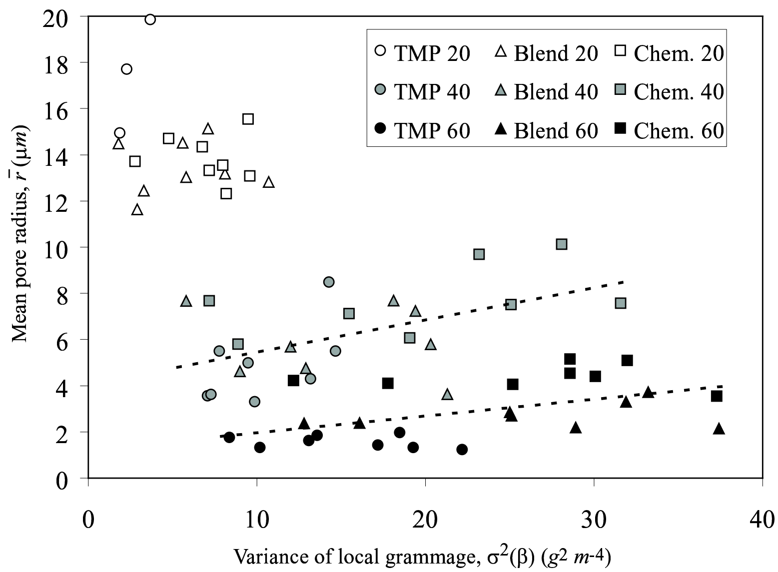

Figure 4: Mean pore radius plotted against variance of local grammage at the 1 mm scale. At 40 and 60 $g\,m^{-2}$ the mean pore radius increases with increasing variance of local grammage.

Influence of formation

Corte and Lloyd [1] used qualitative analysis of formation to infer that the mean, standard deviation and coefficient of variation of pore radii were greater for sheets with poor formation. We have seen that any effect on the coefficient of variation of pore radii is weak and that the standard deviation of pore radii is closely bound to the mean. Accordingly, in our analysis of quantitative relationships between the pore radius distribution and formation, as determined by measurements of contact β-radiographs, we consider only the mean pore radius. Mean pore radii were less than 20 μm for all samples other than the TMP at 20 $g\,m^{-2}$ where there was a high occurrence of pinholes. Also, the relationships observed were very weak at this low grammage for all furnishes considered. in the interest of clarity we therefore consider only samples with mean pore radii less than 20 μm in the plots that follow; these data are typically associated with the sheets formed at 40 and 60 $g\,m^{-2}$.

The mean pore radius is plotted against formation, quantified by the variance of local grammage observed at the 1 mm scale, $\sigma^2(\tilde{\beta})$ in Figure 4. There is considerable scatter to the data and, as might be expected, the data are grouped into three classes determined by their mean grammage; since mean sheet grammage has such a strong influence on the mean pore radius, some of this scatter arises from small departures from the nominal grammage within data groups. Within a given grammage class, the mean pore radius can be seen to increase somewhat with increasing variance of local grammage, *i.e.* worsening formation. The following expressions arise from linear regression of mean pore radius on the variance of local grammage:

$$\begin{aligned} \bar{r} &= 0.140\,\sigma^2(\tilde{\beta}) + 4.041 \qquad \text{for } \bar{\beta} = 40\ g\,m^{-2} \\ \bar{r} &= 0.073\,\sigma^2(\tilde{\beta}) + 1.219 \qquad \text{for } \bar{\beta} = 60\ g\,m^{-2} \end{aligned}$$

with coefficients of determination of 0.277 and 0.254 respectively.

The same data are plotted in Figure 5 with formation quantified by the coefficient of variation of local grammage at the 1 mm scale; the broken line is illustrative only and does not represent any regression on the data. There is little overlap between the data associated with each grammage class reinforcing the observation and expectation that mean sheet grammage has a stronger influence on the pore size distribution than formation. Whilst on first inspection the data for the 40 and 60 $g\,m^{-2}$ sheets seem to form a continuous cluster, within each fibre type and grammage class, there is no strong relationship between the mean pore radius and the coefficient of variation of local grammage.

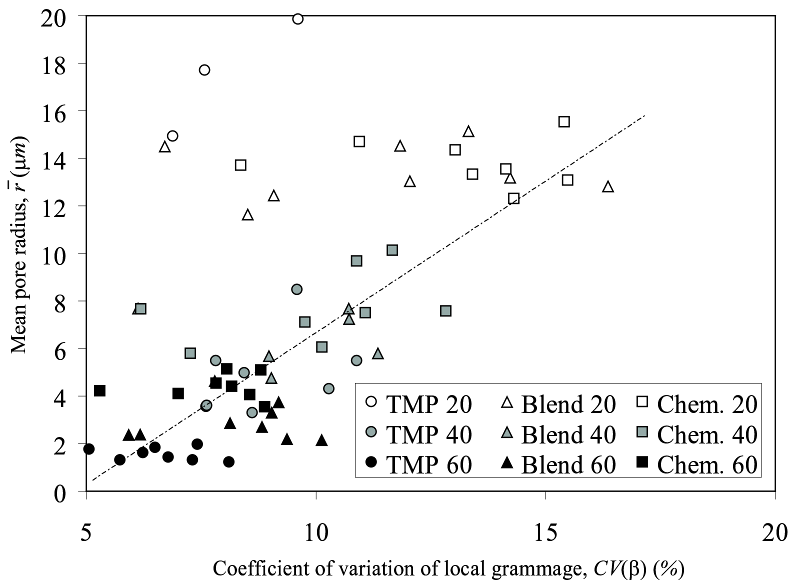

Figure 5: Mean pore radius plotted against coefficient of variation of local grammage at the 1 mm scale. At 40 and 60 $g\,m^{-2}$ the mean pore radius increases with increasing with increasing coefficient of variation of pore radius but fibre type and mean sheet grammage have a stronger effect.

Knowing the morphologies of the fibres as given in Table 1 allowed determination, using the equations of Dodson [14, 15], of the variance of local grammage of a random fibre network formed from the same fibres at the grammages of our samples. The ratio of the measured variance of local grammage at the 1 mm scale to that calculated for a random network yields the *formation number*, n_f at this scale. The mean pore radius is plotted against the formation number in Figure 6. Now, the formation number is dimensionless and factors out changes in mean grammage. Since the mean pore radius is highly sensitive to mean grammage, we observe three grammage dependent classes of data and for the sheets formed at 40 and 60 $g\,m^{-2}$ we see that worsening formation, *i.e.* increasing n_f increases the mean pore radius. Linear regression of mean pore radius on the formation number yields:

$$\begin{aligned} \bar{r} &= 0.544\,n_f + 4.424 \qquad \text{for } \bar{\beta} = 40\ g\,m^{-2} \\ \bar{r} &= 0.592\,n_f + 0.969 \qquad \text{for } \bar{\beta} = 60\ g\,m^{-2} \end{aligned}$$

with coefficients of determination of 0.336 and 0.554 respectively. Note the similar gradients of these regression equations.

Following Farnood *et al.* [16] we used measurements of the variance of local grammage at 100 μm and 200 μm to estimate the mean floc grammage and mean floc diameter. The mean pore radius is plotted against mean floc grammage in Figure 7; a higher floc grammage corresponds to a greater intensity of flocculation. The data for the 40 and 60 $g\,m^{-2}$ sheets in Figure 7 exhibit the following regression:

$$\bar{r} = 4.364\,G - 0.573$$

with coefficient of determination 0.309. Interestingly, the floc grammage is typically higher for the sheets formed at 40 $g\,m^{-2}$ than for those formed at 60 $g\,m^{-2}$. Presumably this is evidence of the evolving pore size distribution being coupled with the evolving mass distribution through preferential drainage effects [17].

Knowing the mean floc grammage and the mean fibre grammage allows determination of a relative floc grammage:

$$\rho_f = \frac{G}{\beta_f} \tag{6}$$

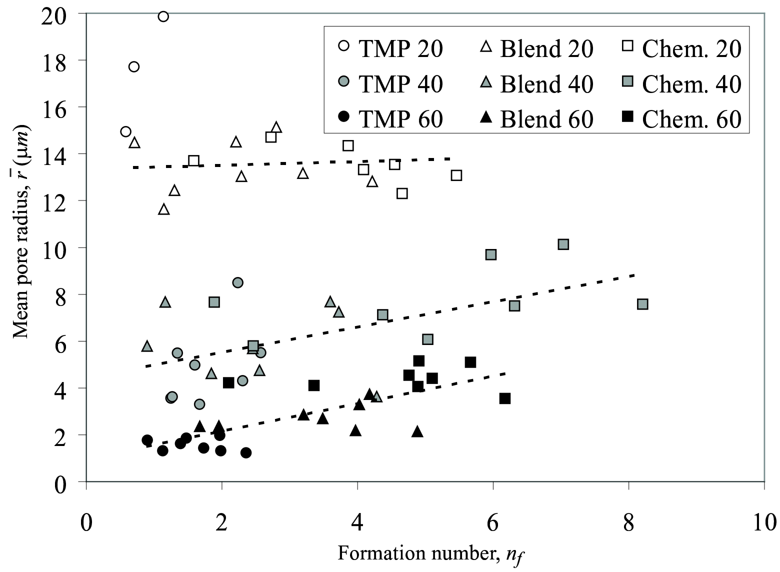

Figure 6: Mean pore radius plotted against formation number at the 1 mm scale. At 40 and 60 $g\,m^{-2}$ the mean pore radius increases with increasing formation number.

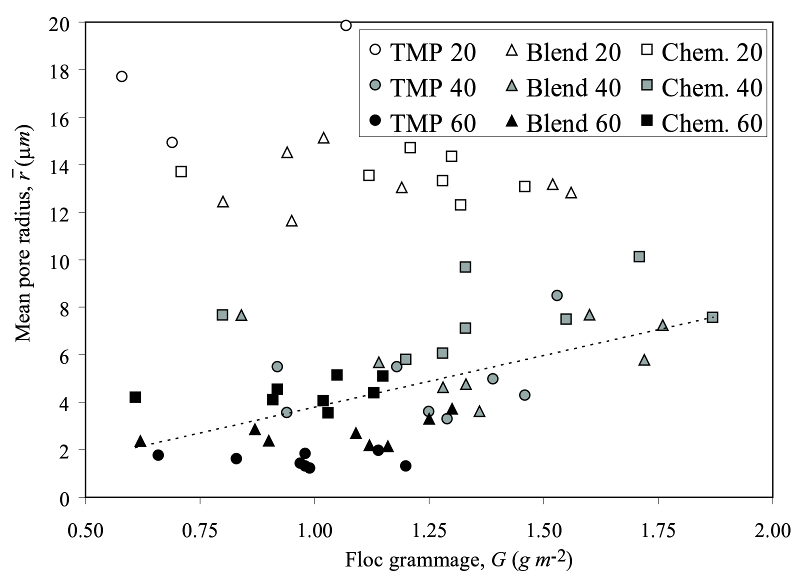

Figure 7: Mean pore radius plotted against floc grammage. At 40 and 60 $g\,m^{-2}$ the mean pore radius increases with increasing floc grammage.

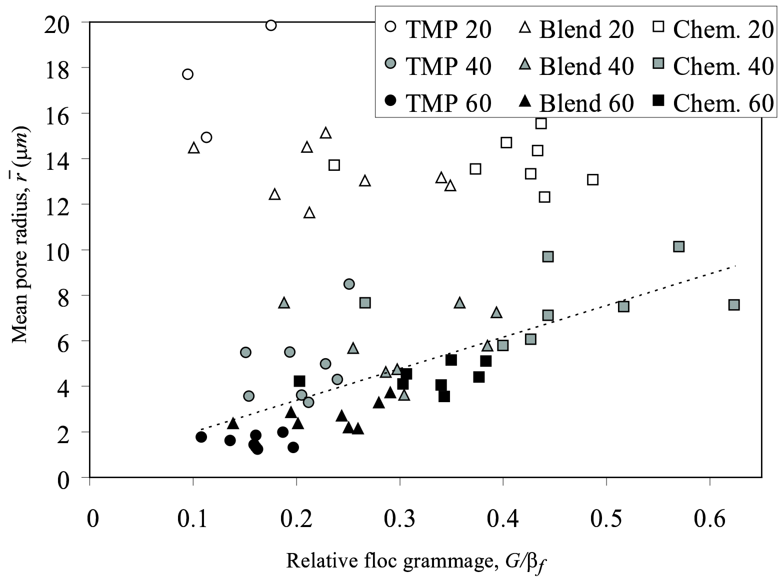

Figure 8: Mean pore radius plotted against relative floc grammage. At 40 and 60 $g\,m^{-2}$ the mean pore radius increases with increasing relative floc grammage; the dependence is stronger than that illustrated in Figure 7.

and we expect $0 \leq \rho_f \leq 1$. The mean pore radius is plotted against this parameter in Figure 8 and regression on the data for the 40 and 60 $g\,m^{-2}$ sheets yields,

$$\bar{r} = 13.922\,\rho_f - 0.586$$

with coefficient of determination 0.497. Whether the relative floc grammage is an appropriate index of formation is open to debate. Nevertheless, of all the formation indices considered here, its correlation with mean pore radius has the smallest residual variance. As discussed previously, some of this residual variance may be associated with small departures of the sheet grammage from the nominal grammage. Also, it should be noted formation analysis was carried out on different areas of larger dimension than the fluid porometry and this would contribute to the scatter in the data.

Conclusions

We have presented experimental data showing that standard deviation of pore radii in paper exhibit the same proportionality for changes in formation and grammage. A consequence of this result is that the coefficient of variation of pore radii is extremely insensitive to these changes and this result provides confirmation of the suitability of the gamma distribution to describe the pore radius distribution in paper. The data confirm that the mean pore radius decreases with increasing grammage and improved formation with the latter being the weaker effect.

References

[1] H. Corte and E.H. Lloyd. Fluid flow through paper and sheet structure. In **Consolidation of the Paper Web** *Trans. IIIrd Fund. Res. Symp.* (F. Bolam, ed.), pp981-1009, BPBMA, London, 1966. See also Discussion following, p 1010.

[2] H. Corte, Bestimmung der Porengrößenverteilung in Papier[1]. *Das Papier* **19**(7):346-351, 1965.

[1] Determination of the pore size distribution in paper

[3] W.C. Bliesner. A study of the porous structure of fibrous sheets using permeability techniques. *Tappi J.* 47 (7):392-400, 1964.

[4] R.E. Miles. Random polygons determined by random lines in a plane. *Proc. Nat. Acad. Sci. USA* **52**:901-907,1157-1160, 1964.

[5] C.T.J. Dodson and W.W. Sampson. The effect of paper formation and grammage on its pore size distribution. *J. Pulp Pap. Sci.* **22**(5):J165-J169, 1996.

[6] J. Castro and M. Ostoja-Starzewski. Particle sieving in a random fiber network. *Appl. Math. Modelling* **24**(8-9):523-534, 2000.

[7] P.R. Johnston. The most probable pore size distribution in fluid filter media. *J. Test. and Eval.* **11**(2):117-121, 1983.

[8] P.R. Johnston. Revisiting the most probable pore size distribution in filter media. The gamma distribution. *Filtrn. and Sepn.* **35**(3):287-292, 1998.

[9] C.T.J. Dodson, Y. Oba, W.W. Sampson. On the distributions of mass, thickness and density in paper. *Appita J.* **54**(4):385-389, 2001.

[10] ASTM Method F316. Pore size characteristics of membrane filters by bubble point and mean (middle) flow pore test.

[11] W.W. Sampson. The structural characterisation of fibre networks in papermaking processes - A review. In **The Science of Papermaking**, *Trans. XIIth Fund. Res. Symp.* (C.F. Baker, ed.), pp1205-1288, Pulp and Paper Fundamental Research Society, Bury, 2001.

[12] W.W. Sampson. Comments on the pore radius distribution in near-planar stochastic fibre networks. *J. Mat. Sci.* **36**:5131-5135, 2001.

[13] T-Y. Hwang and C-Y. Hu. On a characterization of the gamma distribution: The independence of the sample mean and the sample coefficient of variation. *Annals Inst. Statist. Math.* **51**(4):749-753, 1999.

[14] C.T.J. Dodson. Spatial variability and the theory of sampling in random fibrous networks. *J. Roy. Statist. Soc.* **B 33**(1):88-94, 1971.

[15] M. Deng and C.T.J. Dodson. **Paper: An Engineered Stochastic Structure**. Tappi Press, Atlanta 1994.

[16] R.R. Farnood, C.T.J. Dodson and S.R. Loewen. Modelling flocculation. Part I: Random disk model. *J. Pulp Pap. Sci.* **21**(10):J348-J356, 1995.

[17] W.W. Sampson, J. McAlpin, H.W. Kropholler and C.T.J. Dodson. Hydrodynamic smoothing in the sheet forming process. *J. Pulp Pap. Sci.* **21**(12):J422-J426, 1995.